Journal of Visualized Experiments

FRET-measurements in living plant cells

--Manuscript Draft--

Article Type:	Invited Methods Collection - JoVE Produced Video
Manuscript Number:	JoVE62758R2
Full Title:	FRET-measurements in living plant cells
Corresponding Author:	Thorsten Seidel Bielefeld University: Universitat Bielefeld Bielefeld, NRW GERMANY
Corresponding Author's Institution:	Bielefeld University: Universitat Bielefeld
Corresponding Author E-Mail:	tseidel@uni-bielefeld.de
Order of Authors:	Sonja Schmidtpott
	Thorsten Seidel
Additional Information:	
Question	**Response**
Please specify the section of the submitted manuscript.	Biology
Please indicate whether this article will be Standard Access or Open Access.	Standard Access ($1400)
Please indicate the **city, state/province, and country** where this article will be **filmed**. Please do not use abbreviations.	Bielefeld, Germany
Please confirm that you have read and agree to the terms and conditions of the author license agreement that applies below:	I agree to the Author License Agreement
Please provide any comments to the journal here.	

TITLE:

Förster Resonance Energy Transfer Measurements in Living Plant Cells

AUTHORS AND AFFILIATIONS:

Sonja Michele Schmidtpott, Thorsten Seidel

Dynamic Cell Imaging, Biochemistry and Physiology of Plants, Faculty of Biology, Bielefeld University, Bielefeld, Germany

Email address of co-author:

Sonja Michele Schmidtpott (sonja.michele_schmidtpott@uni-bielefeld.de)

Corresponding author:

Thorsten Seidel (tseidel@uni-bielefeld.de)

SUMMARY:

A protocol is provided for setting up a standard confocal laser-scanning microscope for *in vivo* Förster resonance energy transfer measurements, followed by data evaluation.

ABSTRACT:

Sensitized emission-based Förster resonance energy transfer (FRET) experiments are easily done but depend on the microscopic setup. Confocal laser scanning microscopes have become a workhorse for biologists. Commercial systems offer high flexibility in laser power adjustment and detector sensitivity and often combine different detectors to obtain the perfect image. However, the comparison of intensity-based data from different experiments and setups is often impossible due to this flexibility. Biologist-friendly procedures are of advantage and allow for simple and reliable adjustment of laser and detector settings.

Furthermore, as FRET experiments in living cells are affected by the variability in protein expression and donor–acceptor ratios, protein expression levels must be considered for data evaluation. Described here is a simple protocol for reliable and reproducible FRET measurements, including routines for the estimation of protein expression and adjustment of laser intensity and detector settings. Data evaluation will be performed by calibration with a fluorophore fusion of known FRET efficiency. To improve simplicity, correction factors have been compared that have been obtained in cells and by measuring recombinant fluorescent proteins.

INTRODUCTION:

Förster resonance energy transfer ((F)RET) is typically observed by fluorescence spectroscopy, although the process itself is not limited to occur between fluorophores. The underlying dipole-dipole coupling simply requires a light-emitting donor molecule and a light-absorbing acceptor. This is derived from the required spectral overlap integral J of the normalized donor emission and acceptor absorbance spectra[1]. However, because RET competes with fluorescence, the energy transfer becomes measurable by alterations in fluorescence emission: RET induces donor quenching and sensitized acceptor emission.

Fluorophore-based RET has been termed fluorescence resonance energy transfer (FRET) to separate it from bioluminescence resonance energy transfer (BRET). RET depends strongly on the distance between donor and acceptor, which is widely in the range of 0.5–10 nm^2 and thus, in the same range as the dimensions of proteins and their complexes. Second, RET depends on the dipole-dipole orientation kappa squared. Combined with the fact that rotational freedom of protein-bound fluorophores can be neglected due to the molecular weight and the slow rotational relaxation, RET allows for the analysis of conformational alterations[3].

The so-called Förster radius is based on the spectral overlap integral and the wavelength range of the overlap, so that red light-absorbing chromophores result in longer Förster radii than blue light-absorbing dyes. As the dynamic range of FRET measurements is limited by 0.5 × R_0 and 1.5 × R_0, the FRET pair ECFP-EYFP has a dynamic range of 2.5–7.3 nm due to its R_0 of 4.9 nm^4.

The brightness of a fluorophore is given by the product of its molar extinction coefficient and its quantum yield. For FRET measurements, it is advantageous to choose fluorophores of nearly similar brightness. This enhances the detection of donor quenching and sensitized acceptor emission. It also favors the calibration of the microscopy system. Looking at the frequently used FRET pairs of cyan and fluorescent proteins, the lower brightness of the cyan fluorescent proteins becomes obvious (**Figure 1A**).

However, the lifetime of the acceptor must be lower than the lifetime of the donor, ensuring the availability of the acceptor for energy transfer. If the lifetime of the acceptor exceeds the lifetime of the donor, the acceptor might still be in the excited state when the donor is excited again. Advanced cyan fluorescent proteins such as mTurquoise show an extended lifetime and thus contribute to an increased probability of FRET (**Figure1B**). The probability of FRET also depends on the molar extinction coefficient of the acceptor.

PROTOCOL:

NOTE: For the following protocol, transient transfection of protoplasts was performed, as described previously[12]. A brief description is given below.

1. Transient transfection of protoplasts

1.1. Cut ~4 g of healthy leaves of *Arabidopsis thaliana* ecotype Columbia into 1 mm slices and transfer them to 20 mL of enzyme solution (1.5% cellulase; 0.4% macerozyme; 0.1% bovine serum albumin Fraction V; 0.4 M mannitol; 20 mM KCl; 20 mM 2-(*N*-morpholino)ethanesulfonic acid (MES), pH 5.7; 10 mM $CaCl_2$).

1.2. Vacuum-infiltrate the leaf slices with agitation for 2 h at room temperature. Harvest the cells by centrifugation for 3 min at 100 × *g*.

1.3. Wash the protoplasts with W5-solution (154 mM NaCl; 125 mM $CaCl_2$; 5 mM KCl; 2 mM

MES, pH 5.7) and resuspend them in MMG solution (0.4 M mannitol; 15 mM $MgCl_2$; 4 mM MES, pH 5.7).

1.4. Perform the transfection in an 8-well slide by osmotic shock in the presence of polyethyleneglycol (PEG) 4000. Mix 20 µL of the protoplast suspension with 5 µL of plasmid DNA (5 µg/µL) and 25 µL of PEG solution (0.2 M mannitol, 0.1 M $CaCl_2$, 40% PEG 4000).

1.5. Reverse the osmotic shock by gentle readjustment of the osmotic conditions.

NOTE: Besides the sample of interest, the expression of donor alone and acceptor alone is required to determine the spectral bleed-through of the donor and the acceptor, respectively. A fusion protein of the donor and the acceptor must be expressed too for calibration purposes. The fluorescent protein expression was under the control of a cauliflower mosaic virus 35S promoter (pCaMV35S). For all measurements, two confocal laser scanning microscopes (LSM1 and LSM2) were used. LSM1 has two types of detectors: for FRET measurements, the donor signal was detected by a GaAsP-detector, while FRET and acceptor emission were recorded with a photomultiplier. LSM2 has two photomultipliers, which were used for the detection of donor, FRET, and acceptor emission.

2. Laser-adjustment

NOTE: Here, 458 nm and 514 nm lines of an argon-ion laser have been applied for FRET analysis between enhanced cyan fluorescent protein (ECFP)- and enhanced yellow fluorescent protein (EYFP)-labeled proteins. For reproducible data acquisition, both lines were adjusted to similar intensity. This was achieved by either a transmission photomultiplier or the reflection mode.

2.1. Laser adjustment with a transmission photomultiplier

2.1.1. Use an empty well for adjustment.

2.1.2. Choose **line-scanning mode** and **histogram view**.

2.1.3. Decrease the laser intensity to the minimum, and adjust the detector gain to detectable background noise.

2.1.4. Increase the laser intensity in steps of 0.5% and record the corresponding signal.

2.1.5. Apply the routine for both laser lines.

2.2. Laser adjustment with reflective mode

2.2.1. Use an empty well for adjustment.

2.2.2. Apply a reflection filter, switch on the **reflection mode**, if available.

2.2.3. Ensure that the detector wavelength range covers the wavelength of the laser.

2.2.4. Choose the **line-scanning mode** and **histogram view**.

2.2.5. Decrease the laser intensity to the minimum, and adjust the detector gain to detectable background noise.

2.2.6. Move the objective to the lowest position.

2.2.7. Move the objective up until the reflection of the coverslip is visible.

2.2.8. Increase the laser intensity in steps of 0.5% and record the corresponding signal.

2.2.9. Apply the routine for both laser lines.

2.3. Data evaluation

2.3.1. Tabulate the data and sort the data by signal intensities.

2.3.2. Plot the signal intensities against the relative laser power.

2.3.3. Choose laser intensities that result in similar signal intensity.

3. Adjustment of photomultipliers

NOTE: After laser adjustment, the photomultipliers were adjusted to individual gains to obtain similar sensitivity. This calibration was done with the 514 nm laser line, which is in the center of the wavelength range of interest.

3.1. Use an empty well for adjustment.

3.2. Apply a reflection filter, and switch to reflection mode if available.

3.3. Ensure that the detector wavelength range covers the wavelength of the laser (514 nm).

3.4. Choose the **line scanning mode** and **histogram view**.

3.5. Decrease detector gain to half the maximum, and adjust the laser intensity to detectable background noise.

3.6. Move the objective to the lowest position.

3.7. Move the objective up until the reflection of the coverslip is visible.

3.8. Increase the detector gain in steps of 50 to 100 V and record the corresponding signal.

3.9. Apply steps 3.1 to 3.8 for both detectors.

3.10. Data evaluation

3.10.1. Plot the intensity against the detector gain for each detector.

3.10.2. Choose the individual detector gains to obtain similar sensitivity.

4. FRET image acquisition

NOTE: Start with the sample of interest for setting up image acquisition.

4.1. Choose the appropriate filters/dichroic mirrors, e.g., a double dichroic mirror MBS 458/514 for the FRET-pair ECFP/EYFP. Use the same dichroic mirror for all channels to enable line-by-line scanning. Select a water immersion objective for the imaging of living cells. Choose 12 bit- or 16-bit scanning and moderate scanning speed.

4.2. Define the detection range, preferably 470–510 nm for donor detection and 530–600 nm for acceptor/FRET detection in the case of ECFP/EYFP. When using a 445 nm or 440 nm diode laser, use 450 to 510 nm as the detection range. In the case of an acousto-optic beam splitter (AOBS), define donor detection in the range of 450 to 500 nm to prevent unwanted acceptor detection.

4.3. Apply the detector setting according to 3.10.2.

4.4. Apply the laser setting according to 2.3.2. Revise the laser intensity based on the obtained laser power table, if required. Ensure that the signal-to-noise ratio covers the entire dynamic range of the detectors (intensity ranging from 0 to 4095 for 12-bit scanning).

4.5. Keep laser intensities and detector gains constant. Use the pinhole diameter for fine-tuning; keep in mind that changes in the pinhole diameter affect spatial resolution.

4.6. Perform the measurements (take images of at least 20 cells).

5. Determination of crosstalk corrections

NOTE: Cells expressing only the donor or the acceptor are required to determine donor spectral bleed-through (DSBT) and acceptor spectral bleed-through (ASBT), respectively. Keep the same settings described in section 4.

5.1. Perform FRET measurements with cells expressing the donor fluorophore.

5.2. Perform FRET measurements with cells expressing the acceptor fluorophore.

6. Calibration of the measurements according to Beemiller et al.[13]

NOTE: Cells expressing a donor–acceptor fusion of known FRET efficiency are required. Here, an ECFP-5 aa-EYFP-fusion with a FRET efficiency of 0.46 has been used[4]. Keep the same settings described in section 4.

6.1. Perform FRET measurements with cells expressing the donor–acceptor fusion

7. Data evaluation

7.1 Obtain line profiles of the cells, ensuring that each profile contains no more than one cell. Save the profiles as text files.

7.2. Import the text files into a spreadsheet using the **text file import** option in the **Data** section.

7.3. Read out the maximum values by applying the **Max** function.

7.4. List the obtained values in a table, have a column each for donor emission I_D, FRET emission I_F, acceptor emission I_A, and at least four data sets: donor only, acceptor only, donor–acceptor fusion, and measurement.

NOTE: Excitation of the donor also results in direct excitation of the acceptor and causes ASBT that is described by the α value.

7.5. Calculate the ASBT α values with the acceptor-only dataset using equation (**1**).

$$\alpha = \frac{I_F}{I_A} \qquad (\mathbf{1})$$

NOTE: Use the median of all α-values in the following equations. The donor shows a broad emission spectrum that results in emission crosstalk with the sensitized emission of the acceptor. This DSBT is given by the β value.

7.6. Calculate the donor spectral bleed-through β values with the donor-only dataset using equation (**2**).

$$\beta = \frac{I_F}{I_D} \qquad (\mathbf{2})$$

NOTE: Use the median of all β values in the following equations. The calibration factor ξ describes the linear relationship of FRET-derived donor quenching and sensitized emission of the acceptor. Use the medians of 7.5 and 7.6 in the following equations.

7.7. Calculate the calibration factors ξ with the donor–acceptor fusion dataset and its FRET efficiency E (0.46) using equation (**3**).

$$\xi = \frac{I_D E}{(1-E)(I_F - \alpha I_A - \beta I_D)} \quad (\mathbf{3})$$

NOTE: Use the median of all ξ values in the following equations.

7.8. Calculate the FRET efficiencies of the protein pair of interest using equations (**4**) and (**5**).

$$cal.E = \frac{I_D}{(I_F - \alpha I_A - \beta I_D)\xi + I_D} \quad (\mathbf{4})$$

$$E = \frac{I_D}{(I_F - \alpha I_A - \beta I_D) + I_D} \quad (\mathbf{5})$$

7.9. Estimate the effects of expression strength and/or donor–acceptor ratio: plot the sum of I_D, I_F, and I_A against the FRET efficiencies. Perform a linear regression; note that the steeper the graph and the higher R^2 is, the higher is the impact of the expression level or the greater is the difference of donor and acceptor abundance.

REPRESENTATIVE RESULTS:

Adjustment of the confocal laser-scanning microscope

The laser adjustment revealed a linear increase of emission with increasing laser intensity (**Figure 2** and **Table 1**). As expected for argon-ion lasers, the emission of the 514 nm line was much higher than the emission of the 458 nm line, as evidenced by a steeper slope. For subsequent experiments, laser power of 4.5% and 6.5% was chosen for the 514 nm line and the 458 nm line, respectively. This resulted in almost equal emission intensity of 1123 (514 nm) and 1141 (458 nm).

Varying the detector gains at constant laser power revealed an exponential behavior for both analyzed detectors. Similar emission intensities were obtained for a gain of 700 V (**Figure 3**). Although the adjustment of laser lines benefited from the linear behavior, the adjustment of the detectors is likely affected by the exponential behavior, resulting in marked differences with minor changes in the gain at higher voltages. Unfortunately, this higher range is of interest for measurements in living cells, as increasing the laser power is cytotoxic and promotes photobleaching.

Determining spectral bleed-through

At first, the spectral bleed-through of the donor and the acceptor were analyzed with recombinant purified ECFP and EYFP; DSBT β = 0.498 and ASBT α = 0.100. The same was done with cells expressing either ECFP or EYFP. With LSM 2, the estimated DSBT was β = 1.602 ± 0.207 (mean ± SD) and ASBT was α = 0.119 ± 0.018. The median values were β = 1.506 and α = 0.120. This discrepancy between the data obtained in living cells and the data obtained with recombinant protein demonstrates that it is impossible to omit the determination of spectral

bleed-through in living cells. This is likely caused by cellular pigments.

The images reveal the higher brightness of EYFP in comparison to ECFP (**Figure 4** and **Table 2**). Compensating the differences in brightness by different laser settings enhances the dynamic range of the donor and the FRET channel. Providing the relative output by measuring the laser intensities, as done for the adjustment, still increases the reproducibility of the measurements.

For LSM 1, $\beta = 0.171 \pm 0.044$, $\alpha = 0.094 \pm 0.031$ with medians of $\alpha = 0.084$ and $\beta = 0.180$. The determination of the ASBT depends on the laser adjustment and a single detector, and thus, the determination of ASBT performed well. The DBST involves two detectors, resulting in vastly different results for both microscopes. It should be remembered that LSM 2 is equipped with two photomultipliers, whereas LSM 1 uses a GaAsP detector and a photomultiplier, two different types of detectors with different spectral properties and sensitivity. Accordingly, the adjustment works better with two identical detectors.

Calibration of the measurement

For calibration, the median values of α and β were applied, and a fusion of ECFP and EYFP was used as the standard of known FRET efficiency (E = 0.46). The calibration of recombinant and purified ECFP–EYFP resulted in a ξ value of 13.44, while the *in vivo* measurements revealed a ξ value of 1.525 ± 1.844. The median was 0.798, revealing extreme outliers together with the high standard deviation. For LSM 1, the values were $\xi = 1.978 \pm 0.807$ with a median of $\xi = 1.883$. For LSM 2 and LSM 1, the datasets obtained for the calculation of ξ (**Table 3**) were statistically identical, as proven by Student's *t*-test ($p > 0.2$).

FRET measurement

As a proof of concept, the FRET measurement was repeated with the donor–acceptor fusion. The measured FRET efficiency was 0.47 ± 0.07 for the purified protein and 0.47 ± 0.06 in living cells with LSM 2 (**Table 4**). The median of the measurements in living cells was E = 0.45. For LSM 1, the FRET efficiency was 0.46 ± 0.09 with a median of E = 0.45 (**Table 4**). These data demonstrate the effective calibration with a FRET construct of known FRET efficiency.

Effects of expression level and donor–acceptor ratio

For the analyzed data set, the FRET efficiencies were not influenced by the expression level. Due to the fusion of the donor and the acceptor, the ratio was also constant. The inclusion of previous datasets revealed a dependency on the expression level in one case (**Figure 5**). The FRET efficiency between the labeled vacuolar ATPase (V-ATPase) subunits, VHA-A-ECFP and VHA-a-EYFP, decreased with increasing signal intensity. In contrast, the interaction between VHA-E1-ECFP and VHA-C-EYFP was independent of the signal intensity. In the case of VHA-A and VHA-a, the three copies of VHA-A are increasingly replaced by VHA-A-ECFP, which results in a donor excess in comparison to the single copy of VHA-a in the complex. Although VHA-E1 might be present in the form of three copies, the high solubility of VHA-C might abolish this effect in this example. Here, the FRET efficiencies have been comparatively low. This simple approach allows for the testing of expression and ratio artifacts.

FIGURE AND TABLE LEGENDS:

Figure 1: Overview of fluorescent protein FRET pairs with cyan-emitting donors. (**A**) The Förster radii of the pairs and the brightness of donor and acceptor are given for well-characterized FRET pairs. (**B**) Comparison of donor and acceptor lifetimes. Grey asterisks indicate a multiexponential decay. Abbreviations: FRET = Förster resonance energy transfer; CFP = cyan fluorescent protein; GFP = green fluorescent protein; YFP = yellow fluorescent protein; mX = monomeric X; EX = enhanced X; SX = super X.

Figure 2: Laser adjustment. The emission of the lasers was recorded by the reflection of the coverslip and plotted against the relative laser intensity as modulated by the acousto-optic tunable filter of the LSM. Emission of the 458 nm line (**A**) and the 514 nm line (**B**) of an argon-ion laser is shown. Abbreviations: LSM = laser scanning microscope; r.u. = Rayleigh units.

Figure 3: Detector gain and emission intensity. The resulting emission intensities were recorded in the reflection mode for detector gains ranging from 300 to 750 V and 300 to 750 V for detector 1 (**A**) and detector 2 (**B**), respectively. Abbreviation = r.u. = Rayleigh units.

Figure 4: Spectral bleed-through. Images were obtained in the donor, the FRET, and the acceptor channels. (**A**) Images obtained with purified fluorescent proteins; scale bars = 100 µm; (**B**) corresponding images for cells expressing the fluorescent proteins; scale bars = 10 µm. (**C**) Graphs of the obtained SBT values; mean ± SD is given. Abbreviations: FRET = Förster resonance energy transfer; SBT = spectral bleed-through; ECFP = enhanced cyan fluorescent protein; EYFP = enhanced yellow fluorescent protein; LSM = laser scanning microscope; ASBT = acceptor SBT; DSBT = donor SBT.

Figure 5: Effects of expression level and/or donor–acceptor ratio. The sum of the emissions in the donor, FRET, and acceptor channels has been plotted against the FRET efficiency. This has been done for VHA-E1-ECFP and VHA-C-EYFP (**A**), VHA-A-ECFP and VHA-a-EYFP (**B**), and the ECFP–EYFP fusion (**C**). Linear regression was performed; the equation and R^2 are given. Abbreviations: FRET = Förster resonance energy transfer; ECFP = enhanced cyan fluorescent protein; EYFP = enhanced yellow fluorescent protein; VHA = vacuolar ATPase subunit.

Figure 6: Donor and acceptor bleed-through of ECFP and EYFP. The spectra of the fluorescent proteins were obtained from the FP database[14]. (**A**) During sensitized emission experiments, the vast portions of the donor and the acceptor are detected by individual photomultipliers, named PMT1 and PMT2, respectively. ECFP emission is also detectable by the acceptor detector upon excitation with 458 nm. The calculated donor spectral bleed-through into PMT2 is 40.6% of the emission detected by PMT1. (**B**) The emission spectrum of EYFP demonstrates that EYFP shows direct excitation at 458 nm, which is frequently applied for the excitation of cyan donors. The expected excitation efficiency is 9.6% of the excitation at 514 nm. Abbreviations: FP = fluorescent protein; ECFP = enhanced cyan fluorescent protein; EYFP = enhanced yellow fluorescent protein; PMT = photomultiplier.

Table 1: Laser power and signal intensity. The signal intensities of the 458 nm line are given in

blue, the signal intensities of the 514 nm line in green. The intensities applied for the experiment are highlighted in grey.

Table 2: Signal intensities for SBT determination. Recorded maxima and calculated α and β values are given. Abbreviations: SBT = spectral bleed-through; LSM = laser scanning microscope; FRET = Förster resonance energy transfer; ASBT = acceptor SBT; DSBT = donor SBT.

Table 3: Signal intensities for calibration. Recorded maxima and calculated ξ values are given. Corrected values correspond to the FRET signal intensities minus SBT. Abbreviations: SBT = spectral bleed-through; LSM = laser scanning microscope; FRET = Förster resonance energy transfer.

Table 4: Signal intensities for FRET measurements. Recorded maxima and E values are given. Corrected values correspond to the FRET signal intensities minus SBT. Calibrated E values were calculated with calibration by ξ. Abbreviations: SBT = spectral bleed-through; LSM = laser scanning microscope; FRET = Förster resonance energy transfer; cal. = calibrated.

DISCUSSION:

Donor quenching and sensitized acceptor emission are characterized by a linear relationship that allows for either donor- or acceptor-based calculation of FRET. The corresponding factors of linearity are called either G factor (donor to acceptor) or xi (acceptor to donor), which are reciprocal values[4]. Measuring FRET between fluorescent proteins by fluorescence microscopy often requires corrections for DSBT and ASBT due to the broad absorption and emission spectra of the fluorescent proteins. However, many corrections depend on a measurable ASBT, which is a factor in the denominator of the equations in protocol section 7, and an α = 0 results in undefined equations[5,6].

An adjustment of laser intensities is recommended to avoid such effects. This enables the use of acceptor-based calculations and easy detection of inappropriate donor–acceptor ratios. In this protocol, the equation of Beemiller and co-workers has been applied, which has the advantage of simple calibration by a single reference construct of known FRET efficiency. The adjustment of the detectors is critical, especially when two different types of detectors are applied. Previous data obtained with two identical photomultipliers and identical gains resulted in a constant β = 0.61 for multiple experiments over years[7-9] and demonstrate that detector adjustment is advantageous for reproducibility. If the detectors do not allow for a reliable adjustment, a sequential scan with a single detector in a frame-by-frame mode might be an option to avoid bias from detector properties.

Measurements in plant cells are affected by many pigments, which result in excitation light absorption and background autofluorescence. The cellular pigments are mainly excited by light in the UV to blue range[4,10]. This explains the discrepancy between the measurements in cells and those with purified proteins. The purified proteins might serve as a proof of adjustment because the expected values for ASBT α and DSBT β can be derived from the acceptor absorption spectrum and the donor emission spectrum, respectively (**Figure 6**). The values of ASBT are

similar in cells (α = 0.094) and with purified fluorophores (α = 0.114) and close to the expected value of 0.096 due to the low cellular absorption at 514 nm. The DSBT of β = 0.498 with purified proteins is also close to the expected value of 0.406. The spectral bleed-through further depends on the setup; diode lasers of 445 or 440 nm reduce the direct excitation of EYFP and thereby reduce the ASBT. AOBSs are characterized by a smaller transmission gap than dichroic mirrors. Thus, the detection of EYFP is enhanced in the range of 500 to 510 nm and might result in additional ASBT into the donor channel. However, spectral properties of EYFP point to less than 1% emission of the maximum peak, considering both less effective excitation and low emission intensity. The filter gap is much wider with dichroic mirrors, resulting in an additional suppression of such acceptor crosstalk.

However, using the values from purified proteins does not reflect the situation in the cell. The same is true for the calibration by the factor ξ. Although the calibration factor has been similar for both LSM, it was much higher in measurements with the recombinant protein, revealing the impact of cellular pigments. It should be mentioned that in these measurements, the background noise was negligible but detectable and did not affect the observed intensities. In contrast to measurements of the donor lifetime, sensitized emission experiments are sensitive towards the donor–acceptor ratio so that an excess of donor results in decreased FRET efficiency.

However, the protein expression has been under the control of the CaMV35S-promoter in the present experiments. This promoter is frequently used for the overexpression of proteins in plants and might result in unphysiologically high amounts of proteins[13]. Under such conditions, the probability of interaction increases, and false-positive results might occur with higher protein concentrations. Plotting the emission intensities against the FRET efficiency then results in an increasing FRET efficiency with increasing emission intensity and allows for evaluation of the FRET data with respect to the expression level.

It is recommended to separate high-resolution colocalization experiments from FRET measurements. For colocalization, optimal settings are chosen for each fluorophore, while for FRET recording, emission intensities and fine-tuning by the pinhole diameter interfere with optimal image conditions. Nevertheless, the separation of organelles and information on subcellular structures are still encompassed in FRET measurements.

ACKNOWLEDGMENTS:
The experiments were performed at the Light Microscopy Technology Platform (LiMiTec) of the Faculty of Biology, Bielefeld University. This work has been funded by Bielefeld University.

DISCLOSURES:
We ensure that all authors have disclosed any and all conflicts of interest and have no competing financial interests.

REFERENCES:
1. Lakowicz, J. R. *Principles of Fluorescent Spectroscopy*. Third Edition, New York, NY, Springer (2006).

2. Clegg, R. M. Förster resonance energy transfer- FRET what it is, why do it, and how it's done. *Laboratory Techniques in Biochemistry and Molecular Biology*. **33**, 1–57 (2009).

3. Vogel, S. S., Nguyen, T. A., van der Meer, B. W., Blank, P. S. The impact of heterogeneity and dark acceptor states on FRET: implications for using fluorescent protein donors and acceptors. *PLoS ONE.* **7**, e49593 (2012).

4. Müller, S. M., Galliardt, H., Schneider, J., Barisas, B.G., Seidel, T. Quantification of Förster resonance energy transfer by monitoring sensitized emission in living plant cells. *Frontiers in Plant Science.* **4**, 413 (2013).

5. Gadella, T. W. J, van der Krogt, G. N., Bisseling, T. GFP-based FRET-microscopy in living plant cells. *Trends in Plant Science.* **4**, 287–91 (1999),

6. Van Rheenen, J., Langeslag, M., Jalink, K. Correcting confocal acquisition to optimize imaging of fluorescence resonance energy transfer by sensitized emission. *Biophysical Journal.* **86**, 2517–2529 (2004).

7. Seidel, T., Golldack, D., Dietz, K. J. Mapping of C-termini of V-ATPase subunits by *in vivo*-FRET measurements. *FEBS Letters*. **579**, 4374–4382 (2005).

8. Seidel, T., Schnitzer, D., Golldack, D., Sauer, M., Dietz, K.J. Organelle-specific iso-enzymes of plant V-ATPase as revealed by *in vivo*-FRET. *BMC Cell Biology.* **9**, 28 (2008).

9. Schnitzer, D., Seidel, T., Sander, T., Golldack, D., Dietz, K. J. The cellular energization state affects peripheral stalk stability of plant vacuolar H^+-ATPase and impairs vacuolar acidification. *Plant Cell Physiology*. **52**, 946–956 (2011).

10. Roshchina, V. V. Vital autofluorescence: application to the study of plant living cells. *International Journal of Spectroscopy.* 2012, 124672 (2012).

11. Holtorf, S., Apel, .K, Bohlmann, H. Comparison of different constitutive and inducible promoters for the overexpression of transgenes in *Arabidopsis thaliana*. *Plant Molecular Biology*. **29**, 637–646 (1995).

12. Seidel, T. et al. Colocalization and FRET-analysis of subunits c and a of the vacuolar H^+-ATPase in living plant cells. *Journal of Biotechnology*. **112** (1–2), 165–175 (2004).

13. Beemiller, P., Hoppe, A. D., Swanson, J. A. A phosphatidylinositol-3-kinase-dependent signal transition regulates ARF1 and ARF6 during FCγ receptor-mediated phagocytosis. *PLoS Biology*. **4**, e162 (2006).

14. Lambert, T. J. FPbase: a community-editable fluorescent protein database. *Nature Methods.* **16**, 277–278 (2019).

Figure

Click here to access/download;Figure;Figure 1 revised 3 Kopie.eps

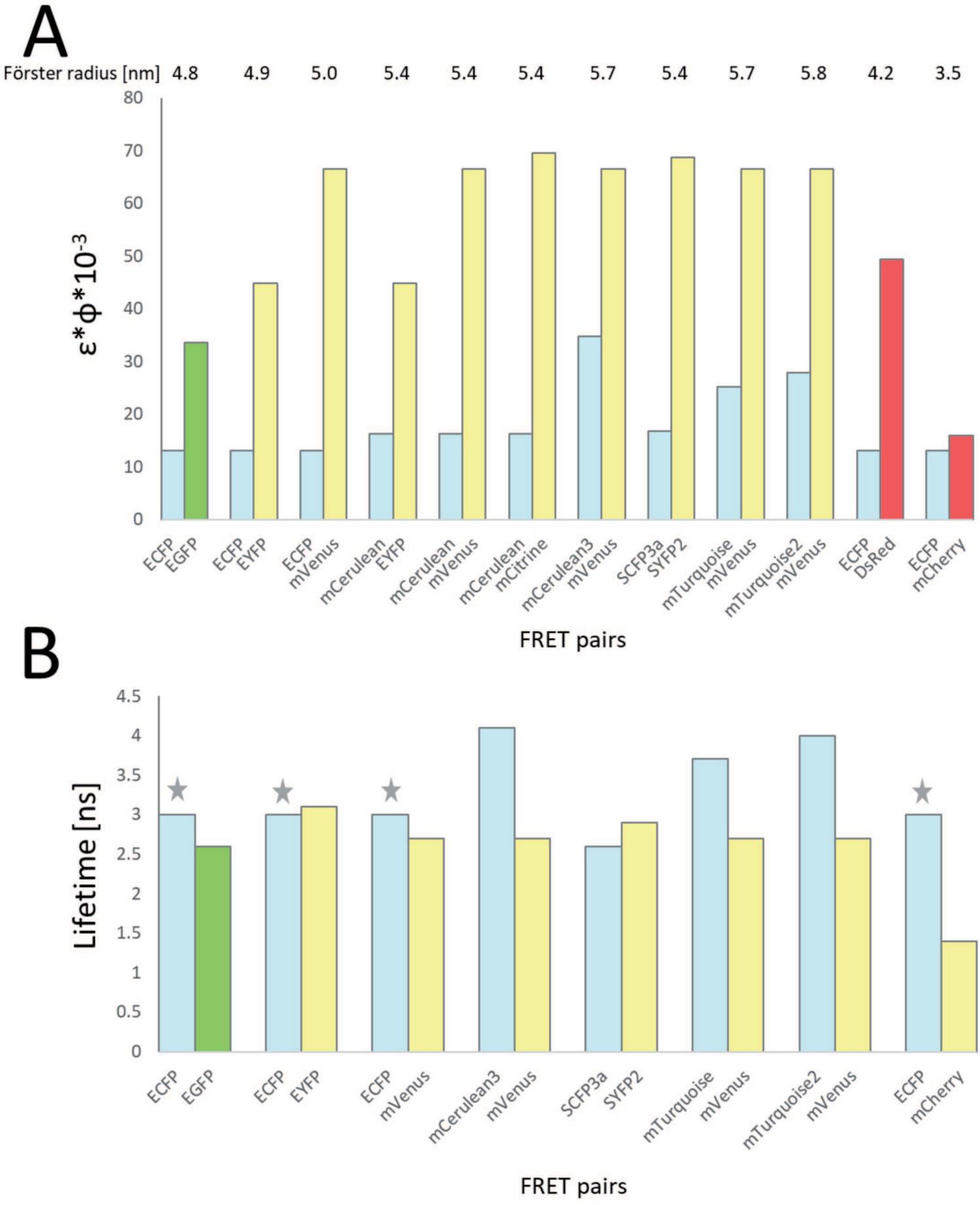

Figure

Click here to access/download;Figure;Figure 2 revised 3 Kopie.eps

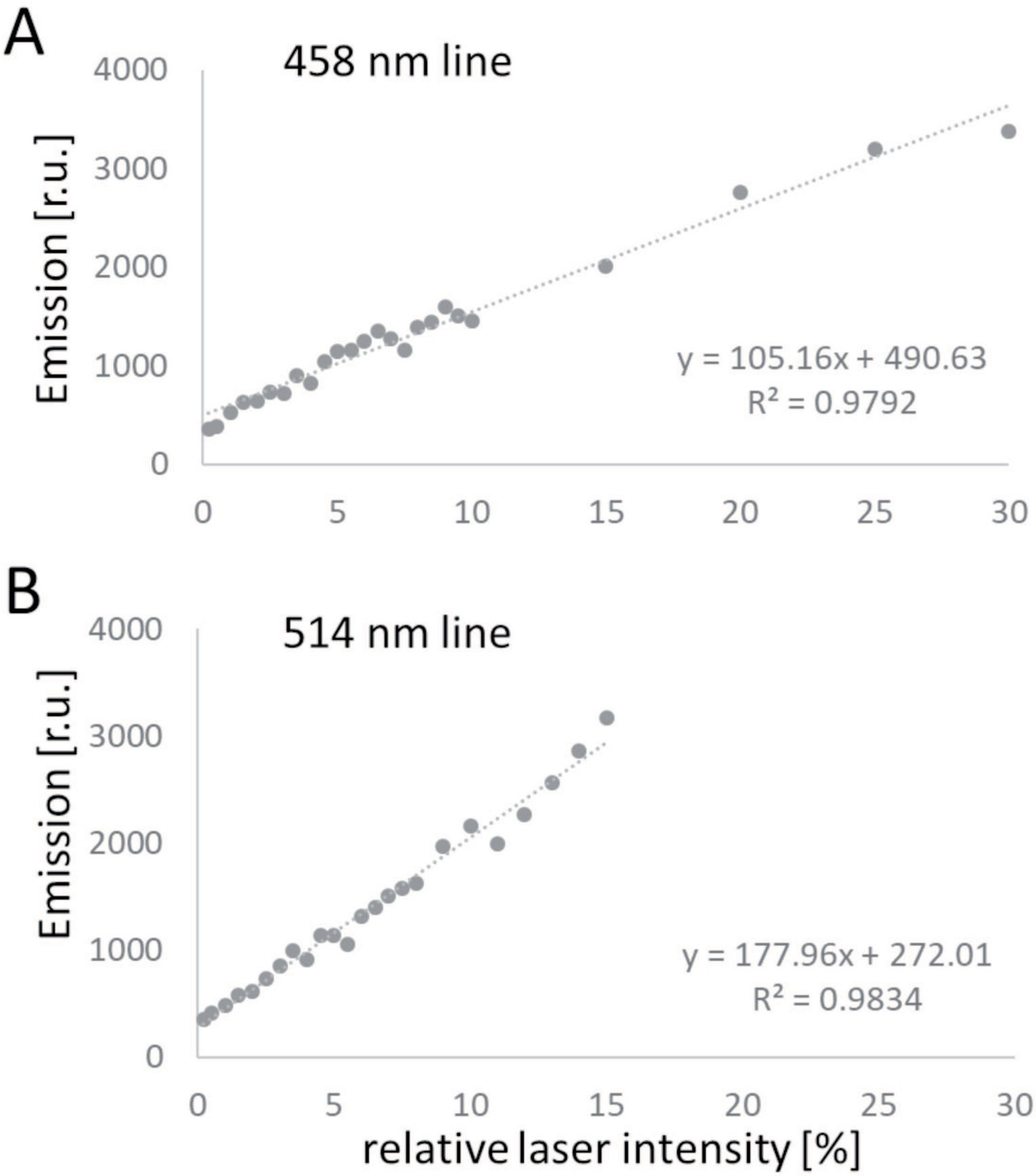

Figure

Click here to access/download;Figure;Figure 3 revised.eps

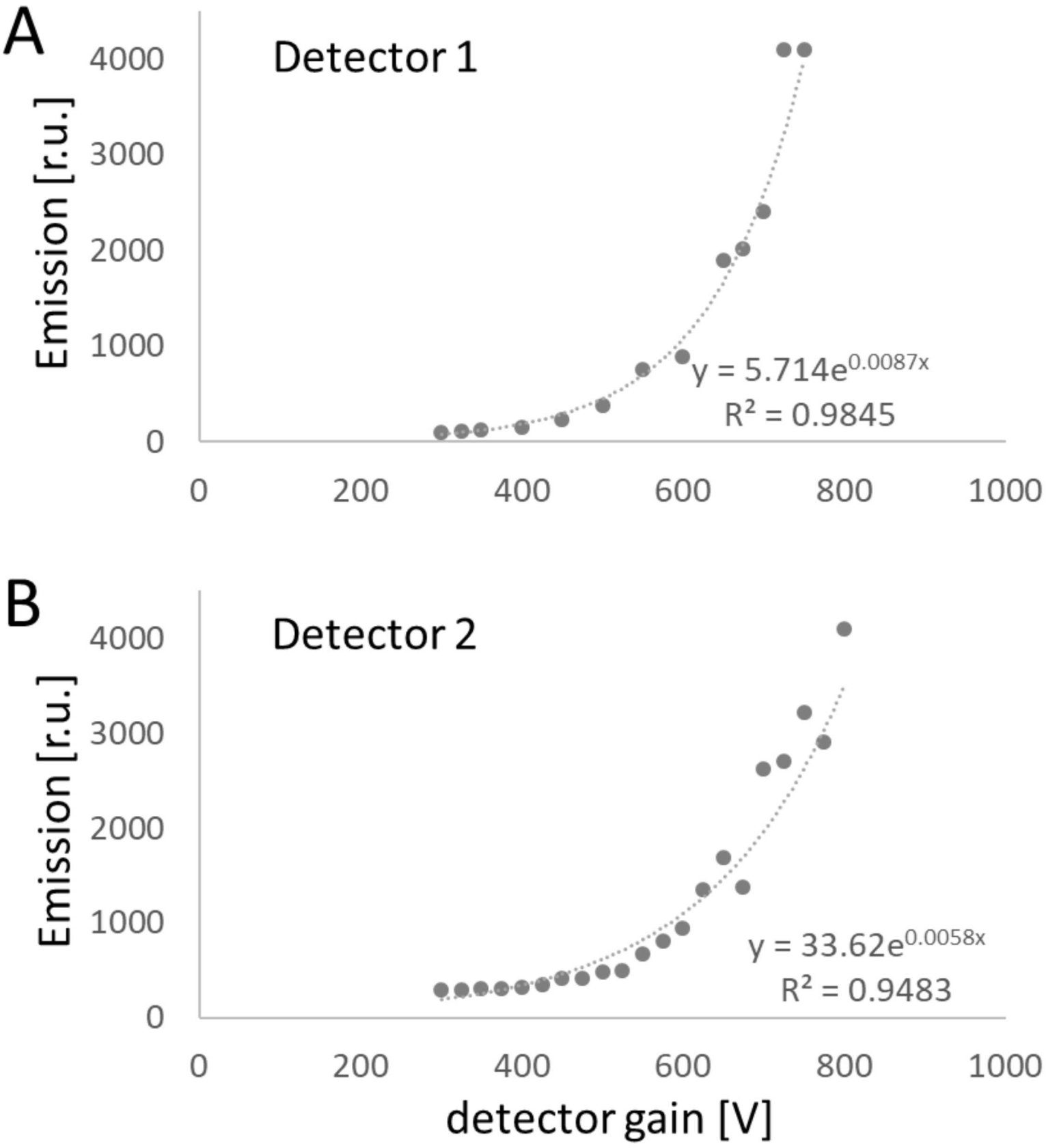

Figure

Click here to access/download;Figure;Figure 4 revised 3 Kopie.eps

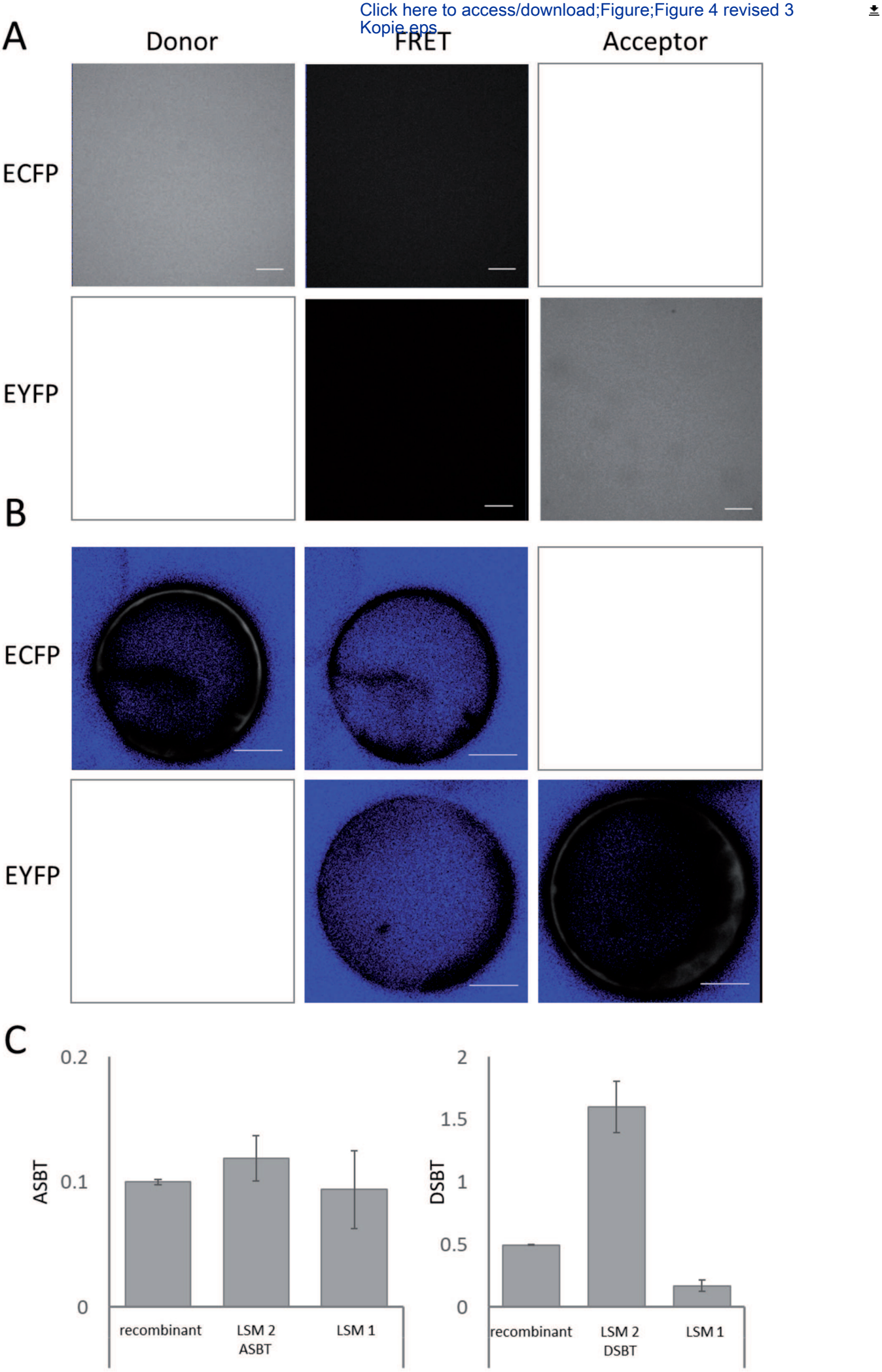

Figure

Click here to access/download;Figure;Figure 5 revised 3 Kopie.eps

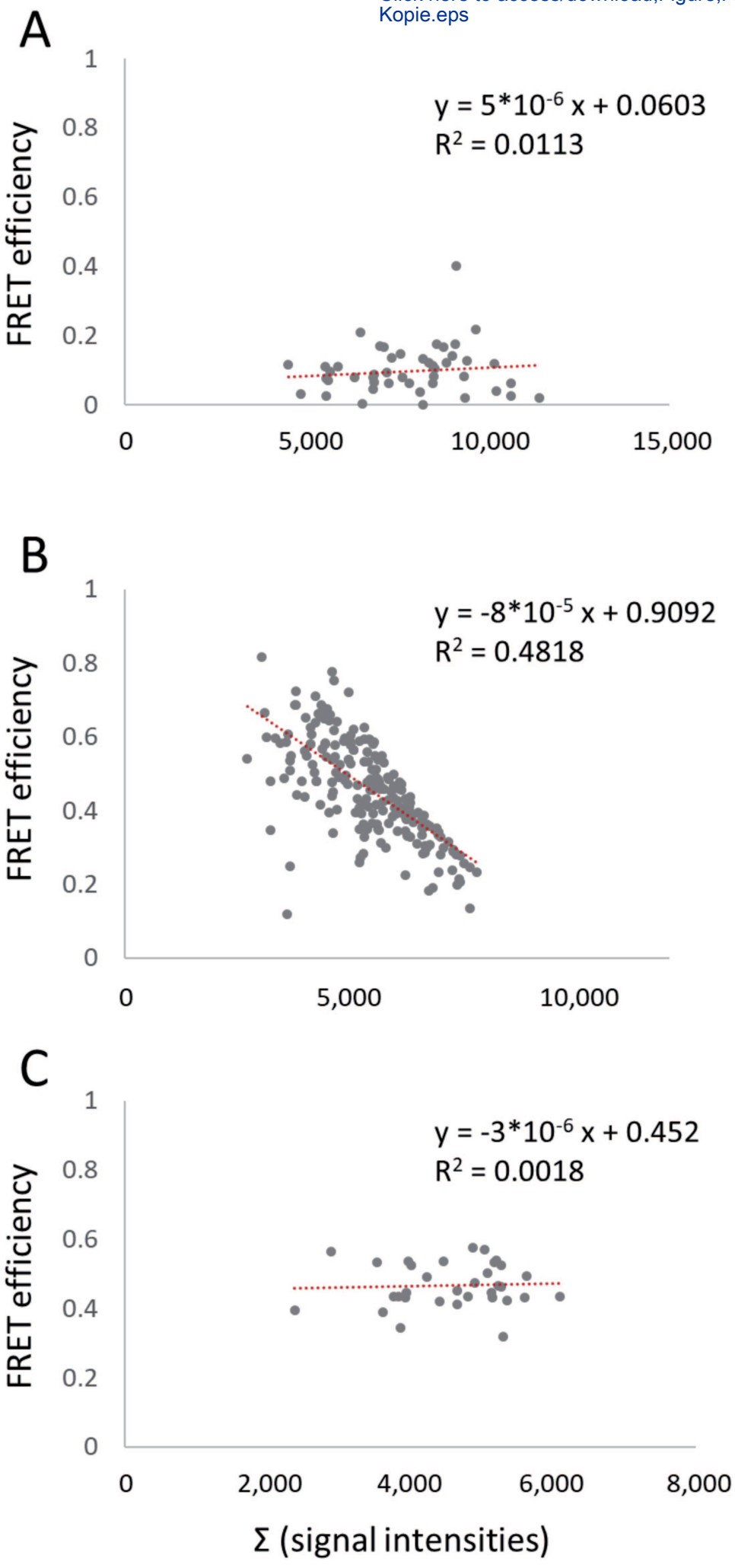

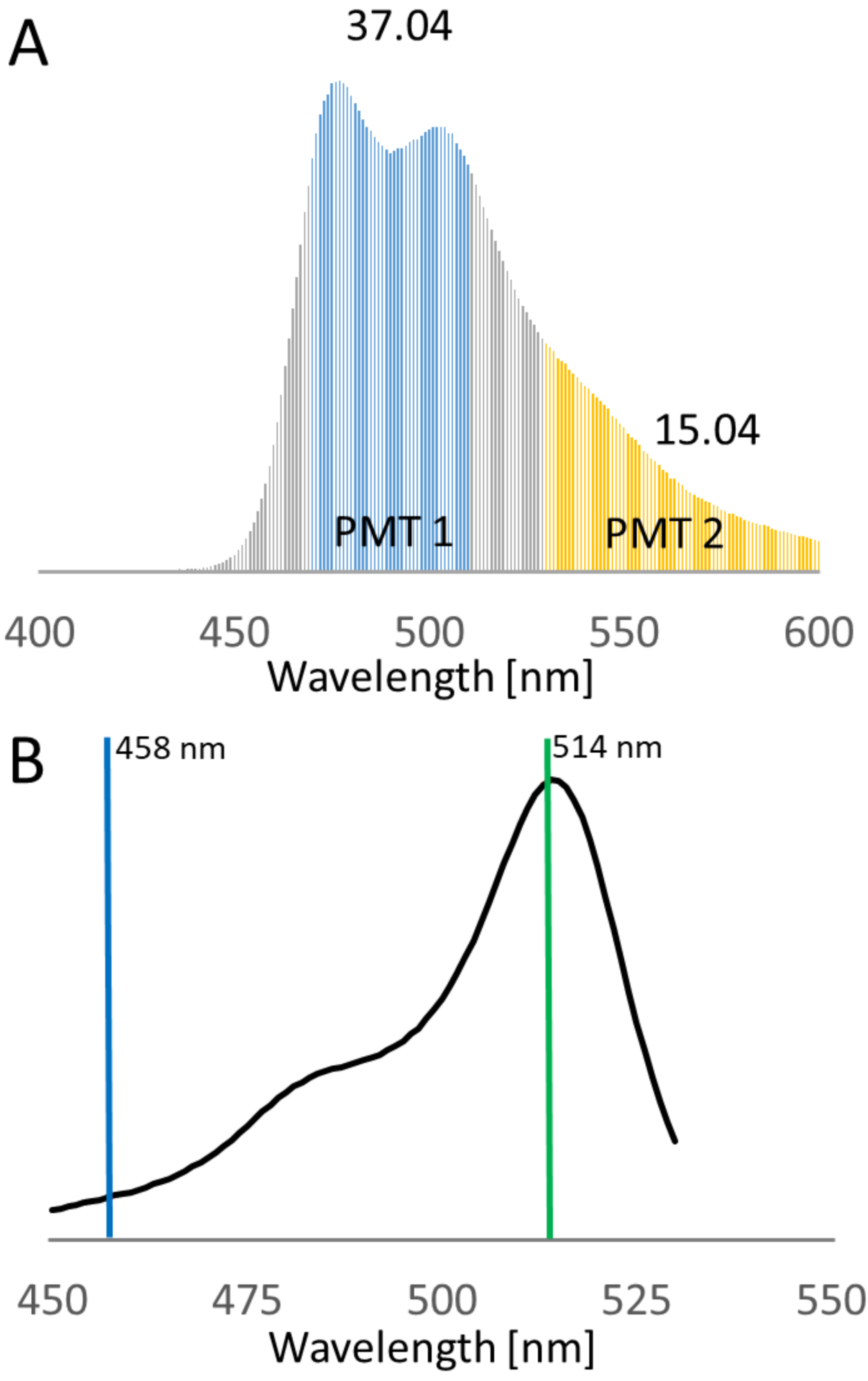

Signal Intensity	Laser power
19	0.2
39	0.5
90	1
132	1.5
171	2
180	0.2
234	2.5
342	0.5
445	3
565	1
622	3.5
721	4
729	1.5
855	4.5
948	2
1095	5
1153	5.5
1223	2.5
1333	3
1567	3.5
1769	4
1840	6
1930	4.5
2060	6.5
2147	5
2167	7
2189	5.5
2600	6
2708	6.5
2718	7.5
2813	8
2898	8.5
3169	7
3284	7.5
3354	9
3424	9.5
3615	8
3914	8.5
3958	10
4095	9
4095	9.5
4095	10

LSM1

FRET	Acceptor	ASBT α
44	525	0.084
65	491	0.132
40	553	0.072
54	667	0.081
31	472	0.066
83	595	0.139
51	564	0.09
104	646	0.161
85	878	0.097
86	1004	0.086
104	875	0.119
64	779	0.082
58	1143	0.051
61	822	0.074
102	1362	0.075

LSM2

FRET	Acceptor	ASBT α
327	3301	0.099
355	2950	0.12
342	3189	0.107
377	3675	0.103
336	3342	0.101
281	2432	0.116
303	3253	0.093
387	3123	0.124
343	3122	0.11
364	2982	0.122
373	2292	0.163
389	3225	0.121
289	2156	0.134
293	2392	0.122
282	1961	0.144

FRET	Donor	DSBT β
235	1226	0.192
148	1434	0.103
339	1513	0.224
284	1831	0.155
337	2012	0.167
294	1431	0.205
188	1334	0.141
173	806	0.215
135	698	0.193
63	639	0.099
142	657	0.216
95	681	0.14

FRET	Donor	DSBT β
486	263	1.848
564	294	1.918
334	204	1.637
263	183	1.437
424	302	1.404
369	245	1.506
334	228	1.465

LSM 1

Donor	FRET	Acceptor	corrected	ξ
698	631	2932	259.92	2.2
981	709	3609	230.36	3.48
552	591	3007	239.85	1.88
587	750	3278	369.85	1.3
824	733	3832	263.86	2.56
562	538	2595	219.59	2.09
560	543	2727	213.88	2.14
1026	1497	4095	969.54	0.87
774	816	3891	350.9	1.8
993	1184	4095	662.47	1.23
644	565	3396	164.73	3.2
746	768	3839	312.28	1.95
791	746	3742	290.33	2.23
421	520	2008	276.1	1.25
520	574	2254	291.71	1.46
538	708	3598	309.84	1.42
569	802	4095	356.61	1.31
464	722	3171	372.91	1.02
684	779	4024	318.91	1.75
655	854	3681	427.87	1.25
628	572	3948	128.34	4
673	655	3577	234.35	2.35
781	713	3920	244.21	2.62
540	605	3513	213.6	2.07
535	743	3952	315.71	1.39
480	651	3820	244.65	1.61
1376	1600	4095	1009.69	1.12
419	496	2764	189.1	1.81
825	888	4089	397.14	1.7
746	764	3881	304.76	2
659	528	3380	126.38	4.27
640	680	3492	272.4	1.92
632	705	4029	253.83	2.04

LSM 2

Donor
418
392
405
283
359
591
271
413
347
374
408
463
345
452
506
474
373
188
190
311
399
318
373
239
290
424
230
196
349
225
483
275
600
580
471
584

FRET	Acceptor	corrected	ξ
776	3827	562.61	0.63
769	3268	530.69	0.63
742	3502	510.74	0.68
405	1495	130.11	1.85
514	2212	202.83	1.51
829	3238	268.72	1.87
648	3157	590.08	0.39
777	2718	439.64	0.8
788	3286	623.83	0.47
718	3612	549.43	0.58
728	3041	437.08	0.8
740	3050	362.15	1.09
617	2478	359.88	0.82
690	2674	285.01	1.35
888	3439	487.64	0.88
851	3610	522.19	0.77
758	3246	547.47	0.58
420	3071	484.65	0.33
293	1804	203.68	0.79
472	2362	255.48	1.04
830	3019	550.86	0.62
630	2304	395.38	0.69
700	2430	392.37	0.81
565	1915	410.49	0.5
752	2584	595.5	0.41
876	3244	583.64	0.62
363	814	91.87	2.13
307	768	84.79	1.97
629	2603	380.36	0.78
415	1281	207.44	0.92
592	1989	55.89	7.36
516	2982	430.86	0.54
715	3079	121.4	4.21
678	2634	63.45	7.79
698	2376	227.14	1.77
692	2745	84.25	5.9

LSM 1

Donor	FRET	Acceptor	corrected	cal. E	E
698	631	2932	259.92	0.41	0.27
981	709	3609	230.36	0.31	0.19
552	591	3007	239.85	0.45	0.3
587	750	3278	369.85	0.54	0.39
824	733	3832	263.86	0.38	0.24
562	538	2595	219.59	0.42	0.28
560	543	2727	213.88	0.42	0.28
1026	1497	4095	969.54	0.64	0.49
774	816	3891	350.9	0.46	0.31
993	1184	4095	662.47	0.56	0.4
644	565	3396	164.73	0.33	0.2
746	768	3839	312.28	0.44	0.3
791	746	3742	290.33	0.41	0.27
421	520	2008	276.1	0.55	0.4
520	574	2254	291.71	0.51	0.36
538	708	3598	309.84	0.52	0.37
569	802	4095	356.61	0.54	0.39
464	722	3171	372.91	0.6	0.45
684	779	4024	318.91	0.47	0.32
655	854	3681	427.87	0.55	0.4
628	572	3948	128.34	0.28	0.17
673	655	3577	234.35	0.4	0.26
781	713	3920	244.21	0.37	0.24
540	605	3513	213.6	0.43	0.28
535	743	3952	315.71	0.53	0.37
480	651	3820	244.65	0.49	0.34
1376	1600	4095	1009.69	0.58	0.42
419	496	2764	189.1	0.46	0.31
825	888	4089	397.14	0.48	0.32
746	764	3881	304.76	0.43	0.29
659	528	3380	126.38	0.27	0.16
640	680	3492	272.4	0.44	0.3
632	705	4029	253.83	0.43	0.29

LSM 2

Donor	FRET	Acceptor	corrected	cal. E	E
449	859	3816	594.7	0.52	0.57
321	566	2056	297.06	0.43	0.48
413	730	3554	492.13	0.49	0.54
269	388	1319	114.56	0.26	0.3
599	829	3238	255.92	0.26	0.3
372	504	2212	172.03	0.27	0.32
369	787	3428	604.53	0.57	0.62
340	578	2276	304.84	0.42	0.47
402	661	2681	336.84	0.4	0.46
368	716	3040	488.96	0.52	0.57
414	826	3472	576.77	0.53	0.58
356	572	2120	254.68	0.37	0.42
480	854	3826	541.29	0.48	0.53
372	766	3349	569.33	0.55	0.6
464	849	3788	557.37	0.49	0.55
336	731	2434	483.05	0.54	0.59
354	821	2627	567.21	0.56	0.62
366	688	2379	385.5	0.46	0.51
333	614	2622	393.22	0.49	0.54
263	732	2610	621.79	0.66	0.7
249	508	1749	317.73	0.51	0.56
388	761	3340	537.66	0.53	0.58
214	357	886	120.03	0.31	0.36
228	331	719	51.76	0.16	0.19
215	323	872	82.77	0.24	0.28
452	602	1948	110.61	0.17	0.2
460	571	1802	49.44	0.08	0.1
625	722	3079	88.4	0.1	0.12
618	721	2848	71.11	0.09	0.1
522	630	2768	124.19	0.16	0.19
553	644	2775	89.43	0.12	0.14
462	620	2335	158.67	0.22	0.26
478	564	2186	59.33	0.09	0.11

Dear Editor,

We have revised the manuscript and responded to all comments of the reviewers. We were somewhat surprised by the first reviewer who suggests to revise the manuscript so that it exclusively works with Leica microscopes, as a consequence of the technical improvements he/she demanded. However, we have considered his/her points of criticism, but kept the protocol in a general, brand-independent way. We hope we can convince you with the revised manuscript.

Best regards,

Thorsten and Sonja

Changes to be made by the Author(s):
1. Please take this opportunity to thoroughly proofread the manuscript to ensure that there are no spelling or grammar issues. Please define all abbreviations at first use.

Hopefully we defined them all now.

2. For in-text formatting, corresponding reference numbers should appear as numbered superscripts after the appropriate statement(s), but before punctuation.

Done.

3. Why is RET the abbreviation for Förster resonance energy transfer in line 37?

We have added an “F” in brackets. It is RET for the basic process, FRET for fluorescence and BRET for bioluminescence.

4. Please revise the text, especially in the protocol, to avoid the use of any personal pronouns (e.g., "we", "you", "our" etc.).

Done.

5. Please ensure that all text in the protocol section is written in the imperative tense as if telling someone how to do the technique (e.g., “Do this,” “Ensure that,” etc.). The actions should be described in the imperative tense in complete sentences wherever possible. Avoid usage of phrases such as “could be,” “should be,” and “would be” throughout the Protocol. Any text that cannot be written in the imperative tense may be added as a “Note.” However, notes should be concise and used sparingly. Please include all safety procedures and use of hoods, etc.

We have revised the manuscript, eliminated all “should” and “could”.

6. The Protocol should contain only action items that direct the reader to do something. Please move the discussion about the protocol (lines 69-88) to the introduction or Discussion.

The discussion has been moved and follows directly the introduction.

7. Please note that your protocol will be used to generate the script for the video and must contain everything that you would like shown in the video. Please ensure you answer the "how" question, i.e., how is the step performed? Alternatively, add references to published material specifying how to perform the protocol action. There should be enough detail in each step to supplement the actions seen in the video so that viewers can easily replicate the protocol.

Checked and revised.

8. Please format the manuscript as: paragraph Indentation: 0 for both left and right and special: none, Line spacings: single. Please include a single line space between each step, substep and note in the protocol section. Please use Calibri 12 points and one-inch margins on all the side. Please include a one line space between each protocol step and then highlight up to 3 pages of protocol text for inclusion in the protocol section of the video.

Checked. To not exceed three pages, the calculations were omitted from the video.

9. Some of your references are incomplete; please ensure that the references appear as the following: [Lastname, F.I., LastName, F.I., LastName, F.I. Article Title. Source (ITALICS). Volume (BOLD) (Issue), FirstPage–LastPage (YEAR).] For 6 and more than 6 authors, list only the first author then et al. Please include volume and issue numbers for all references, and do not abbreviate the journal names.

Has been revised.

10. Please include a scale bar for all images taken with a microscope to provide context to the magnification used. Define the scale in the appropriate Figure Legend (e.g., Fig 4).

Scale bars has been defined in the legend (Fig. 4).

11. All tables should be uploaded separately to your Editorial Manager account in the form of an .xls or .xlsx file. Please make sure that decimals appear as periods and not commas in the tables and figures and anywhere else in the manuscript.

Done.

12. Please ensure that the Table of Materials contains a comprehensive list of essential supplies, reagents, and equipment. The table should include the name, company, and catalog number of all relevant materials in separate columns in an xls/xlsx file. Please sort the Materials Table alphabetically by the name of the material.

Revised.

_____

We are grateful to all reviewers for their valuable and helpful comments. Please find our response in red next to the comments.:

Reviewers' comments:

Reviewer #1:

Journal of Visualized Experiments
FRET-measurements in living plant cells
Sonja Schmidtpott
Thorsten Seidel

This paper describes a protocol for intensity-based FRET measurements in living plant cells. I reject this paper as I disagree with many aspects listed in this paper. The authors state to calibrate laser lines and photomultipier tubes for FRET measurements. In my opinion to determine FRET using sensitised emission it is important to adjust the microscope as such that reliable signals are obtained, which requires identical imaging settings. In this paper, the authors use 2 microscopes and these two microscopes have either GasP of PMTs. For quantitative FRET measurements one should use detectors like Hybrid detectors that are able to read signal in photon counting mode. The whole calibration with detectors is truly not necessary as FRET is a ratiometric method. Furthermore, detailed description on how the measurements were done is not provided; image properties, mode of recording, scan speed etc.

We have included a recommendation for 12- or 16-bit scanning, line-by-line scanning and moderate scan speed. “moderate”, because setting the scan speed is different for the various LSM-programs and depends on the manufacturer.

Hybrid detectors are specific for Leica LSMs such as the SP8 or later models. We do not want to suggest a protocol, which is brand-specific. Photon counting is also not available for all confocal laser-scanning microscopes.

Remarks
Line 57: The brightness of a fluorophore is given by its absorption co-efficient and its quantum yield. I would say it is the product of molar extinction coefficient and quantum yield.

We have revised the sentence as suggested.

Line 58 For FRET-measurements, it is of advantage to choose fluorophores of nearly similar brightness. Again, to me it is not necessary to have this, for intensity based FRET it is handy to have an acceptor that has bright like YFP, but you can use mCherry as well as is shown in publications. I wonder why the authors show in their paper the FRET using ECFP and EYFP as a FRET pair. This is definitely not a very good FRET pair as many new variants have appeared, yielding higher R0 and thereby obtaining higher FRET.

It has not been our intention to go for the best FRET-pair. We wanted to suggest a protocol that even works for less optimal pairs, the more since ECFP and EYFP are still frequently used.

Line 62 On the other hand, the lifetime of the acceptor should be lower than the lifetime of the donor, ensuring the availability of the acceptor for energy transfer. Maybe the authors can explain this to me. It is important to have a donor with long lifetime, so it is longer in the excited state and possibly undergo FRET. Acceptors need to have high molar extinction coefficient.

Two points of view: 1) The donor increases the probability of energy transfer by a long lifetime. 2) in a 1:1 ratio of donor and acceptor or an excess of donor the donor would already be ready to emit or transfer energy, when a long-lifetime acceptor is still in the excited state. This prevents energy transfer and decreases the probability.

Line 146: Define the detection range, we recommend 470 - 510 nm for donor detection and 530 - 600 nm for acceptor/FRET detection in case of ECFP/EYFP. I disagree to select donor emission up to 510 nm as a small fraction of YFP is captured at that wavelength as well. I recommend using 440 nm laser and select a window for cyan coloured proteins between 450-495 nm.

Looks again like you are used to a Leica SP8. This is true for systems with an AOBS and the pulsed 440 nm laser typical for Leica, but again it is not our intention to suggest the optimal equipment and a protocol that only works with the system of one manufacturer. We want to suggest a protocol for a standard confocal with dichroic mirrors and argon-ion lasers. However, we have included a recommendation that pays attention to the now sold 445 (440) nm diode laser instead of the argon-ion laser and to the usage of an AOBS. With dichroic mirrors you will not get any detectable acceptor signal at 500 – 510 nm, since spectral properties point to less than 1% emission of the maximum peak, considering both less effective excitation and low emission. Furthermore, the filter gap is much wider with the dichroic mirror than with an AOBS, resulting in an additional suppression of acceptor crosstalk.

Line 152: keep laser intensities and detector gains constant. Use the pinhole diameter for fine-tuning. Adjusting pinhole for getting similar intensities is new for me, lose significant resolution….

We have included “keep in mind that changes of the pinhole diameter affect spatial resolution”. Using the pinhole for fine-tuning, you do not lose much of resolution and still ensure separation of organelles and subcellular structures. Furthermore, we strictly separate high-resolution co-localization experiments from interaction studies by FRET.

Figure 2 shows the emission vs laser percentage, but usually micro-Watt is plotted on X-axis. This shows that the AOTF has linear dependency.

Thank you for this more precise suggestion. The legend has been revised.

Line 224 The spectral bleedthrough is shown. With LSM2 the DSBT is 1.6, meaning the donor only has a higher signal in acceptor channel compared to donor channel. This observation you obtain if you keep all the laser and detector setting similar. As mentioned before, use photon counting for reliable read-out.

Please read the sentence again. This DSBT is valid for measurements in cells, but not for the recombinant fluorescent protein. This discrepancy is already addressed in the manuscript. We moved this comment closer to the statement, so that it becomes clearer.

Reviewer #2:
Manuscript Summary:
This paper describes a protocol on confocal-based sensitised-emission FRET in living plant cells. The protocol provides plenty of detail and explanations which will enable readers / users with a basic microscopy background to apply the described techniques themselves in a successful manner. I endorse this submission for publication.

Major Concerns:
no major concerns

Minor Concerns:
The labelling of the figures, graphs and tables is insufficient. Readers would appreciate if some of the information from the legends was presented in the figures/tables/graphs as well (such as Figure 3A; also state "detector 1" and in Fig 3B "detector 2).

Thank you for this suggestion, we have revised the figures.

Or in Fig 4C, the columns are labelled with LSM5 or LSM780, but these instruments are always referred to as LSM1 or LSM2 in the protocol. It would make sense not to mix the names.

Sorry for that, we missed to correct the names in the figure. It is revised now.

Authors should not use the term "spectra" as singular; please use the term "spectrum" instead (line 301: "The emission spectrum of EYFP...").

Revised.

In table 1, please highlight the intensity values/laser powers that were used in the protocol (see line 212-213).

Done.

In the section 6 "Data evaluation", please describe the parameters more precisely, such as: alpha-values describe acceptor bleedthrough caused by direct excitation of the acceptor at the donor excitation wavelength or beta-values describe emission cross-talk by the donor (that is just an example; I am sure the authors can do better);

We have revised the protocol.

describe IA=fluorescence intensity of the acceptor, ID=fluorescence intensity of the donor, et cetera.

The definition is available in 6.4.

In line 220, I would say that ..."increasing the laser power is cytotoxic and promotes photobleaching". In line 246, I personally think that the standard deviation (1.525+/-1.844) reveals the outliers.

Both have been revised, thank you!

Reviewer #3:
Manuscript Summary:
FRET-measurements in living plant cells is a detailed protocol that provides a worked example of how to measure emission-based FRET between ECFP-EYFP tagged proteins transiently expressed in Arabidopsis mesophyll protoplasts. This method has been successfully utilized by the authors in number of studies whose results are well-published. Therefore, according to the intent, the authors have written a biologist-friendly procedure of high quality. The adjustment of the confocal microscope setup before the routine acquisition, representative results, calculations and data evaluation are clearly described in a step-by step manner. The introduction provides also an overview of the palette of currently used fluorescent proteins (FPs) for FRET measurements including characterization of fluorescence lifetime for each FP. An advantage of this protocol is that can be adapted to the available standard confocal laser-scanning microscope and for other fluorophore pair then ECFP-EYFP. From my point of view, this protocol will be of great interest for plant biologists working in the area of protein-protein interaction in living plant cells.

Minor comment:
Please, unify Figures referencing style (Figure or Fig.) in the text main body.

Done.

Thank you for your support!